ACS APPLIED MATERIALS & INTERFACES

Research Article

www.acsami.org

Role of Hydrogen Plasma Pretreatment in Improving Passivation of the Silicon Surface for Solar Cells Applications

Fengyou Wang,[†] Xiaodan Zhang,*[,†] Liguo Wang,[†,‡] Yanjian Jiang,[†] Changchun Wei,[†] Jian Sun,[†] and Ying Zhao[†]

[†]Institute of Photo-electronics Thin Film Devices and Technique of Nankai University, Key Laboratory of Photo-electronics Thin Film Devices and Technique of Tianjin, Key Laboratory of Photo-Electronic Information Science and Technology of Ministry of Education (Nankai University), Tianjin 300071, China

[‡]Institute of Information Functional Materials, Hebei University of Technology, Tianjin 300130, China

ABSTRACT: We have investigated the role of hydrogen plasma pretreatment in promoting silicon surface passivation, in particular examining its effects on modifying the microstructure of the subsequently deposited thin hydrogenated amorphous silicon (a-Si:H) passivation film. We demonstrate that pretreating the silicon surface with hydrogen plasma for 40 s improves the homogeneity and compactness of the a-Si:H film by enhancing precursor diffusion and thus increasing the minority carrier lifetime (τ_{eff}). However, excessive pretreatment also increases the density of dangling bond defects on the surface due to etching effects of the hydrogen plasma. By varying the duration of hydrogen plasma pretreatment in fabricating silicon heterojunction solar cells based on textured substrates, we also demonstrate that, although the performance of the solar cells shows a similar tendency to that of the τ_{eff} on polished wafers, the optimal duration is prolonged owing to the differences in the surface morphology of the substrates. These results suggest that the hydrogen plasma condition must be carefully regulated to achieve the optimal level of surface atomic hydrogen coverage and avoid the generation of defects on the silicon wafer.

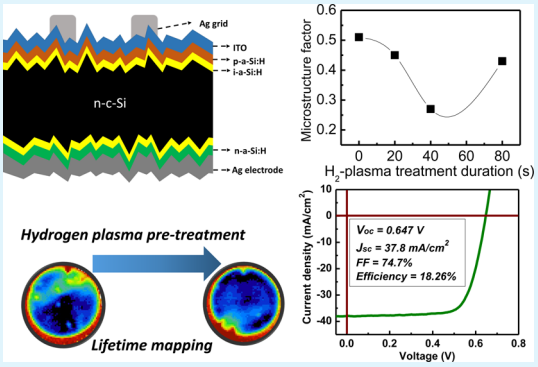

KEYWORDS: *hydrogen plasma, surface passivation, microstructure, solar cells, minority carrier lifetime*

1. INTRODUCTION

Silicon heterojunction (SHJ) solar cells, which consist of hydrogenated amorphous silicon (a-Si:H) and crystalline silicon (c-Si), form a potentially inexpensive alternative to standard p−n homojunction c-Si solar cells because of their low-temperature production processes with less chances of device degradation and their superior temperature coefficients.[1−6] The key factor to the high performance of the SHJ solar cell is the a-Si:H/c-Si heterointerface, because the features of the interface directly affect the junction properties and hence the outputs of solar cell.[7−13] The silicon surface could be well passivated by introducing an intrinsic a-Si:H (i-a-Si:H) film as a passivation layer before depositing the doped emitter layer on the front side and the back surface field (BSF) layer on the rear side. The passivation properties of the i-a-Si:H films have been widely studied, and various laboratories have obtained excellent results based on float zone silicon wafers, using different deposition techniques.[14−16] Schulze et al.[17] found that cells with a device-quality buffer layer showed better performance than those with a buffer layer deposited at higher temperatures with inappropriate levels of hydrogen and higher defect density. In addition, surface passivation can also be achieved with a pretreatment of atomic hydrogen.[18−23] Martín et al.[21] have used the hydrogen plasma treatment for p-type silicon wafers, and their experimental results show that hydrogen plasma treatment improves surface passivation. They suggest that a possible origin of the improved passivation may be the removal of additional contaminants like hydrocarbons from the surface. In addition, the reconstruction of the silicon surface have been considered as another use of the hydrogen plasma treatment,[22,23] but its influence on the subsequently deposited thin film passivation layer has not been investigated. Kim et al.[24] found that the decrease in the silicon surface recombination velocity after hydrogen plasma treatment was caused by the increased hydrogen concentration at the silicon surface. Although the results described above suggest that surface treatment by hydrogen plasma promotes device performance, the mechanism by which hydrogen plasma pretreatment improves surface passivation of c-Si remains unclear, especially for SHJ solar cells applications. Therefore, as a prerequisite to extensive application of the this technique, it is an important issue to clarify precisely how the hydrogen plasma pretreatment impacts SHJ solar cells and to analyze the appropriate corresponding process.

Accordingly, in this study, we used the hydrogen plasma pretreatment process before depositing the i-a-Si:H films in

Received: May 22, 2014
Accepted: August 20, 2014
Published: August 20, 2014

Table 1. RF-PECVD System Conditions for Hydrogen Plasma Pretreatment and i-a-Si:H Films

process	T_{dep} (°C)	H_2 (sccm)	SiH_4 (sccm)	thickness (nm)	power density (mW/cm^2)	pressure (Torr)
H_2-plasma treatment	140	50			8	2.2
i-a-Si:H	140	50	20	10	25	1

Table 2. Conditions During RF-PECVD in the Fabrication of Solar Cells

layer	P (mW/cm^2)	T_{dep} (°C)	p (Torr)	SiH_4 (sccm)	TMB (sccm)	PH_3 (sccm)	H_2 (sccm)
p-a-Si:H	53	180	2	1	2		120
n^+-a-Si:H	53	180	1.3	2		2.5	180

order to improve the passivation effects of the c-Si surface. In contrast to the investigations mentioned above, our approach focused on the treatment of the c-Si surface before i-a-Si:H deposition, and we investigated the influence of the hydrogen plasma on regulating the a-Si:H microstructure as a function of treatment duration. Moreover, the power density and pressure were intentionally set low (8 mW/cm^2) and high (2.2 Torr), respectively, to provide a sufficient flux density of hydrogen atoms with low kinetic energy but without excessive bombardment of the c-Si substrate.[25] We demonstrate that hydrogen plasma pretreatment promotes the homogeneity and compactness of the i-a-Si:H film, which thus improves the τ_{eff} value. Notably, a surface diffusion mode was proposed to offer a much more detailed explanation of the effect of hydrogen plasma pretreatment. On the basis of this work, SHJ solar cells were fabricated, and their performance characteristics were then analyzed by varying the duration of hydrogen plasma pretreatment.

2. EXPERIMENTAL SECTION

2.1. Substrate Preparation. Czochralski (Cz) grown chemically−mechanically polished ⟨111⟩ n-type phosphorus-doped monocrystalline silicon samples (250 ± 10 μm thick) with a resistivity of 1−3 Ω cm were used in the present study. As a predeposition surface cleaning step, the samples were treated with acetone/methanol/deionized water and then subjected to the RCA cleaning procedure. Then, the samples were immersed in a H_2SO_4/H_2O_2 (3:1) solution for 5 min to grow a chemical oxide and rinsed in deionized water for storage. Before a-Si:H deposition, the native oxide was removed from the wafer by dipping it into 1% hydrofluoric acid for 3 min. After blow-drying with nitrogen, the samples were immediately transported to the load lock of the deposition system to avoid oxidation or other contamination.

2.2. Hydrogen Plasma Pretreatment and a-Si:H Film Deposition. The hydrogen plasma pretreatment was conducted by radio frequency plasma enhanced chemical vapor deposition (RF-PECVD) at 13.56 MHz in a high vacuum multichamber cluster deposition system. The plasma exposure time was varied from 0 to 90 s. After hydrogen plasma pretreatment, i-a-Si:H layers with a thickness of 10 nm were deposited bifacially, using a mixture of SiH_4 and H_2 at the substrate temperature (T_{dep}) of 140 °C and prepared in the same chamber. Details of the plasma pretreatment and i-a-Si:H deposition conditions are listed in Table 1. The passivation qualities were measured by using quasi-steady-state photoconductance (QSSPC) and microwave photoconductance decay (μ-PCD) systems. The injection level of the excess carrier density for μ-PCD is 10^{13} cm^{-3}. The microstructure of the a-Si:H films was characterized by measurements obtained with Fourier transform infrared spectroscopy (FTIR) in the attenuated total reflectance (ATR) mode to analyze the effects of hydrogen plasma pretreatment.

2.3. SHJ Solar Cell Fabrication. SHJ solar cells were fabricated on n-type tetramethylammonium hydroxide (TMAH)-textured 280 μm-thick Cz silicon wafers. The cells were structured as follows: Ag grid/indium tin oxide (ITO)/p-a-Si:H/i-a-Si:H/n-c-Si/i-a-Si:H/n-a-Si:H/Ag back contact. The p-a-Si:H and n-a-Si:H films were prepared in two separate chambers of the PECVD system at 180 °C. The p-a-Si:H films were prepared with gaseous mixtures of silane (SiH_4), trimethylboron (TMB), and H_2. The n-a-Si:H films were prepared with gaseous mixtures of SiH_4, phosphine (PH_3), and H_2. Details of the deposition conditions for p- and n-a-Si:H films are provided in Table 2. The Ag grid (~600 nm thick), Ag back contact (~600 nm thick), and ITO layers (~80 nm thick) were prepared by physical vapor deposition (PVD) and patterned onto the 1 cm^2 pad area. The current density−voltage (J−V) characteristics of the solar cells were measured at 25 °C under 1 sun (AM1.5, 100 mW/m^2) of radiation from a solar simulator.

3. RESULTS AND DISCUSSION

Figure 1 shows the minority carrier lifetime (τ_{eff}) of samples based on polished and textured substrates with a 10 nm i-a-Si:H

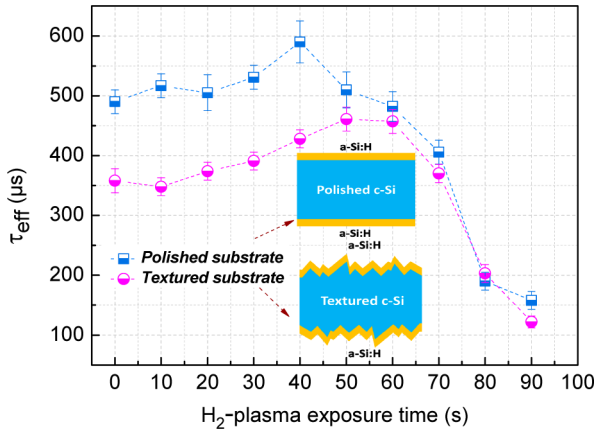

Figure 1. τ_{eff} values of the textured and polished substrates plotted as a function of hydrogen plasma treatment duration. The inset shows a schematic diagram of the sample structure.

layer plotted as a function of the duration of hydrogen plasma pretreatment. The τ_{eff} value was measured by QSSPC with an injection level of 10^{15} cm^{-3}. Without the hydrogen plasma pretreatment, the τ_{eff} value of the sample based on polished wafer was 490 μs. As the duration of hydrogen exposure increased, the τ_{eff} increased to 40 s and then decreased. Moreover, the τ_{eff} value of the samples based on textured substrates have a similar tendency, but the optimal duration is prolonged. Intuitively, the increase in τ_{eff} due to the hydrogen plasma treatment is usually considered to result from (1) removal of residual oxides, (2) cleaning of the wafer surface,[26] or (3) passivation of surface defects. Mechanism (1) requires that oxidation must occur, and mechanism (2) requires that there be a high plasma discharge power density. However, because we carefully and immediately transported the silicon wafer from the hydrofluoric acid solution to the vacuum deposition system (10^{-7} Pa) and the discharge power density

dx.doi.org/10.1021/am5031837 | ACS Appl. Mater. Interfaces 2014, 6, 15098−15104

was low, it is worth wondering whether there is some other primary reason for the increase in τ_{eff} other than residual oxide removal or wafer surface cleaning by hydrogen plasma pretreatment. To test whether the mechanism (3) (passivation of surface defects by hydrogen) is the sole reason for this effect and clarify the role of hydrogen plasma treatment, we need a comprehensive understanding of the passivation characteristics of the samples, not just the lifetime values but also the distribution of passivation on the wafer. Therefore, four representative samples (A, B, C, and D) were selected, and μ-PCD measurements of the samples were made and compared.

Details of the exposure time and the corresponding average τ_{eff} of these samples are presented in Table 3. The results of the

Table 3. Exposure Time and Average τ_{eff} Values of Different Samples

sample	duration (s)	average lifetime (μs)
A	0	174.73
B	20	233.09
C	40	229.16
D	80	121.90

average lifetime obtained from μ-PCD measurements show a tendency similar to that of QSSPC measurements, although the values are lower than the QSSPC measurements owing to the lower level of excess carrier injection (at 10^{13} cm^{-3}) for μ-PCD measurements.[27] Figure 2 shows the spatial distribution maps of the lifetime as measured by using μ-PCD for samples A to D; the histograms in Figure 2a–d show the surface ratios (S_r) for different lifetime values to quantitatively evaluate the uniformity of the passivated wafers. S_r is defined as $S_r = [S_n]/[S_{wafer}]$, where S_n is the surface area associated with a narrow range of lifetime values (corresponding to the range of lifetimes in one of the bins in the histograms in Figure 2) and S_{wafer} is the entire area of the silicon wafer. Therefore, if the S_r value of one histogram is higher for a certain lifetime range and lower for others, this indicates that the lifetime distribution of this sample is uniform.

Figure 2 shows that, as the pretreatment duration increased, passivation became more uniform up to a duration of 40 s, after which the uniformity deteriorated. Notably, although the average lifetime of sample D is less than that of the shorter hydrogen plasma pretreatment samples, the S_r of the histogram in Figure 2d for the range of 150–160 μs is clearly prominent; moreover, the lifetime map of sample D also reveals that passivation is more homogeneous than that for samples A or B. This suggests that the hydrogen plasma pretreatment could improve the passivation homogeneity although the excessively long treatment duration will worsen the passivation effect.

On the basis of these findings, we propose that the c-Si surface passivated promotion hydrogen plasma pretreatment is attributed to the improvement of the uniformity and microstructure of a-Si:H films in addition to the aforementioned reasons. Since the homogeneity of the ultrathin a-Si:H is directly influenced by the structure of the film, samples A–D were characterized ex-situ by ATR-FTIR spectroscopy.

Figure 3 shows the stretching bands of samples in the range of 1840–2260 cm^{-1}. The FTIR curves do not have a large

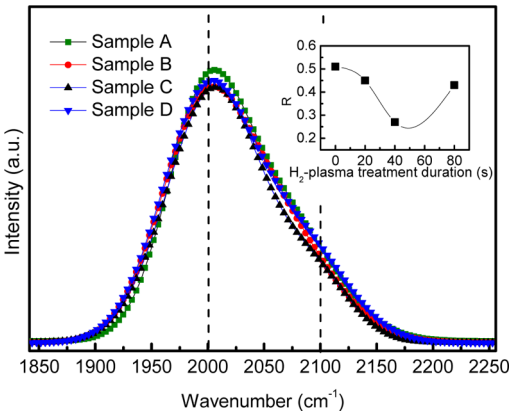

Figure 3. ATR-FTIR spectra and R (inset) of samples with different hydrogen plasma pretreatment durations.

margin difference in this range. Due to the quite thin amorphous silicon films (~10 nm), the signal intensity is weak. Thus, the peak area (I_{2000}, I_{2100}) of the curves will be more sensitively determined by the Y axis intensity; i.e., there will be a great change even when the intensity has a little drift. Generally, double-Gaussian-function fitting peaks near 2000

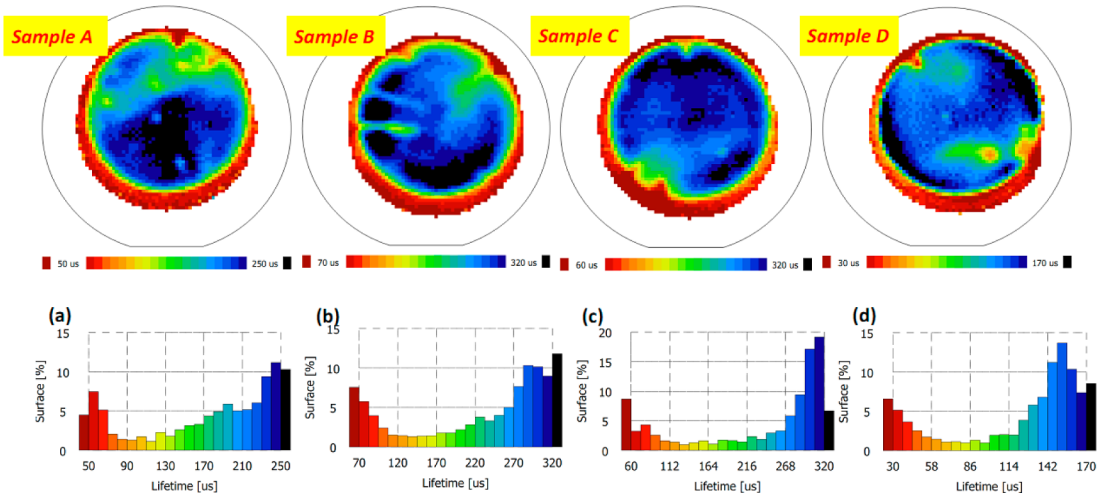

Figure 2. Minority carrier lifetime measured by using μ-PCD for different samples. (a–d) The S_r distribution as a function of lifetime for samples A–D to quantitatively evaluate the uniformity of the passivated wafers.

cm^{-1} for monohydride (SiH) bonds and 2100 cm^{-1} for higher hydride (SiH_2) bonds are used to analyze such spectra.[28] The microstructure factor of the a-Si:H film, marked as R in the figure (i.e., the ratio of the area of the SiH_2 peak to that of the SiH peak, such that $R = I_{2100}/(I_{2100} + I_{2000})$), reflects the compactness and bulk quality of the film. The smaller the R value, the better the bulk quality of the a-Si:H film (i.e., the more compact the structure of the a-Si:H film). The ATR-FTIR results show that both the SiH_2 bond content (at 2100 cm^{-1}) and the R in the samples (plotted in the inset of Figure 3) decrease as the exposure time increases to 40 s, after which they increase. Schulze et al.[29] showed that the as-deposited interface defect density is determined by the local and nonequilibrated network structure at the a-Si:H/c-Si interface. Achieving high quality (i.e., a compactly structured a-Si:H film with fewer defects) will improve the τ_{eff} value of the passivated wafer. Therefore, for insufficient or excessive pretreatment exposure times, the microstructure and network of the subsequently deposited a-Si:H films are richer in voids and defects. These low-quality and inhomogeneous films were unable to provide sufficient passivation effects for c-Si. Hence, the τ_{eff} of the samples decreased. These results suggest that the hydrogen plasma pretreatment modifies the microstructure of the deposited a-Si:H film, increases the homogeneity and compactness of the a-Si:H films, and thereby improves the τ_{eff}. However, excessively long pretreatment with hydrogen plasma also increases the density of dangling bond defects on the surface owing to the etching effects of hydrogen plasma,[20,30] increases the R value of the a-Si:H films, and hence reduces the τ_{eff} values of the samples.

To clarify how the passivation effect of a-Si:H films is improved by hydrogen plasma pretreatment, we further propose a surface diffusion model. Although similar models have generally been employed to describe the formation of microcrystalline silicon thin films fabricated by the PECVD process,[31,32] they are not completely identical to the model proposed here. Initially, to avoid the risk of epitaxial growth of the a-Si:H film on the c-Si substrate, the substrate temperature was set to only 140 °C. The surface diffusion coefficient (D_s) can be expressed by the following expression:

$$D_s \propto a^2 \exp(-E_s/kT) \quad (1)$$

where a is the jump distance between the adsorption sites, E_s is the activation energy for a surface-diffusion jump, k is the Boltzmann constant, and T is the temperature.[33] Therefore, a low substrate temperature will reduce the D_s value of the a-Si:H film precursors and result in the microstructure of the a-Si:H film being more disordered with an atomically inhomogeneous surface. The surface diffusion model stresses the significance of the surface coverage by hydrogen, over which film precursors diffuse more easily. In our process, as shown in Figure 4a, hydrogen plasma pretreatment with a sufficient flux density of atomic hydrogen realizes full surface coverage by bonded hydrogen. Such coverage of the surface by bonded hydrogen saturates the dangling bonds and enhances the surface diffusion length. As a consequence, as shown in Figure 4b, the a-Si:H film precursors (SiH_3) that are subsequently adsorbed on the surface can achieve energetically favorable (stable) sites, leading to the formation of an atomically flat surface and improving the level of a-Si:H film passivation. However, the hydrogen plasma pretreatment is also associated with local heating through hydrogen-recombination reactions on the silicon wafer surface which will break the Si−Si bonds[34,35] and generate defects on the silicon wafer, which is detrimental for the surface passivation. However, this process was associated with local heating effects caused by hydrogen recombination at the silicon surface. The local heating effects were conducive to an increase in the diffusion coefficient of the a-Si:H precursors on silicon substrate, which could compensate the homogeneity to a certain extent even though dangling bond defects are generated. The underlying principle of hydrogen plasma pretreatment can be illustrated by the following reactions.[36]

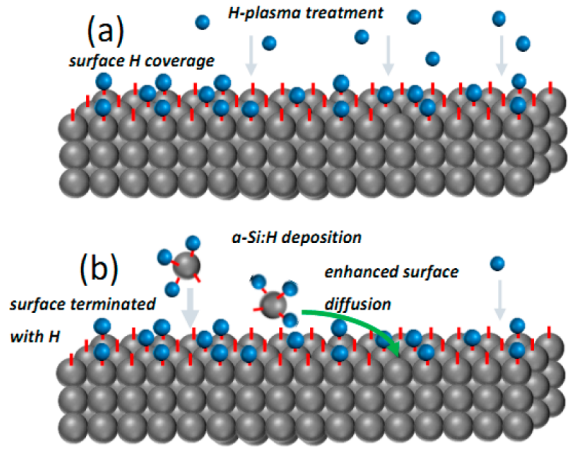

Figure 4. Schematic drawing of (a) a bare silicon surface treated with hydrogen plasma and (b) the resultant intrinsic a-Si:H deposition.

$$H_{(g)} + Si^- \rightarrow SiH \quad (2)$$

$$H_{(g)} + SiH \rightarrow H_2 + Si^- \quad (3)$$

$$H_{(g)} + Si{-}Si \rightarrow SiH + Si^- \quad (4)$$

The rate of each reaction depends on the surface coverage or local concentration of the reacting species, which are Si^-, Si−Si, and SiH, respectively. For the initial hydrogen plasma pretreatment phase, the c-Si wafers, from which native oxide had been removed by hydrofluoric acid, were covered with large amounts of Si^-; thus, reaction 2 was dominant. This contributed to an increase in the amount of SiH, which helped to enhance the surface diffusion length. As plasma exposure increased, reaction 3 gradually became the predominant factor because of the increasing number of SiH molecules; furthermore, reaction 4 also accompanied reaction 3 during this hydrogen abstraction process. Therefore, the c-Si wafer surface again exhibits the exposure of more silicon dangling bonds. These considerations suggest that sufficient hydrogen coverage of the silicon surface is obtained without generating additional defects on the c-Si surface only under a suitable range of treatment durations.

Finally, in accord with the results mentioned above, we used the hydrogen plasma pretreatment process to fabricate SHJ solar cells based on textured substrates. The structure of the SHJ solar cell is shown in Figure 5a. Figure 5b shows the $J-V$ characteristics for solar cells pretreated with hydrogen plasma for 60 s, exhibiting a conversion efficiency of 18.26%. Because the excellent surface passivation of c-Si is a key prerequisite to yield a high V_{oc} and a high efficiency,[37] we plotted in Figure 5c the output parameters of solar cells prepared with various hydrogen plasma exposure times while keeping the other parameters constant (see Table 2 for the parameter values). Both FF and V_{oc} show trends similar to that of the τ_{eff} (Figure

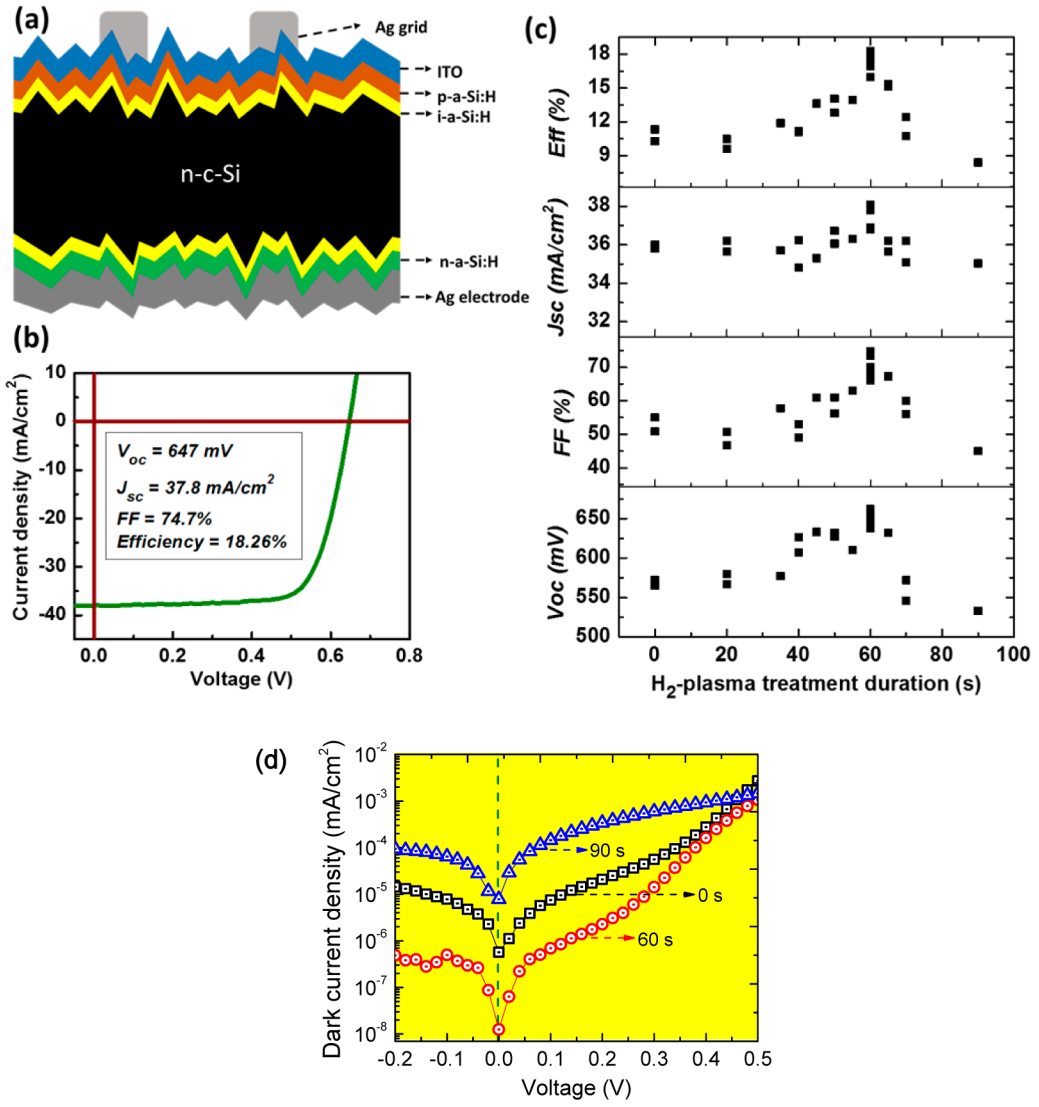

Figure 5. (a) Schematic diagram of the SHJ solar cell. (b) Illuminated $J-V$ characteristics of the SHJ solar cell with a 60 s H_2 plasma treatment. (c) Output parameters plotted as a function of the duration of the hydrogen plasma treatment. (d) Dark $J-V$ characteristics of the SHJ solar cells with 0, 60, and 90 s H_2 plasma treatment, respectively.

1). The FF value of the solar cells is apparently more sensitive to the treatment duration because it is impacted not only by τ_{eff} but also by the uniformity and roughness of the a-Si:H/c-Si interface. Figure 5d has shown the dark $J-V$ characteristics of the solar cells treated with different durations to diagnosis the shunting path within the p−n junction. When the H-plasma pretreatment duration was 60 s, the dark current curve of the solar cell at forward bias voltage (<0.5 V) is lower compared with the one without treatment. Further prolonging the duration to 90 s, the dark current shows a more significant increase. On the basis of the semiconductor device physics, the increase of the dark current at low forward bias voltage is directly related to the increase of the depletion region recombination and shunting path within the p−n junction. Besides, the electrical current of the p−n junction under reverse bias voltage also indicates that the device fabrication with a 60 s hydrogen plasma pretreatment has more leakage current within the p−n junction. These results indicate that an inhomogeneous interface is likely to increase carrier recombination and shunting currents, which should decrease the parallel resistance of the device and thus reduce the FF of the solar cells. Figure 6

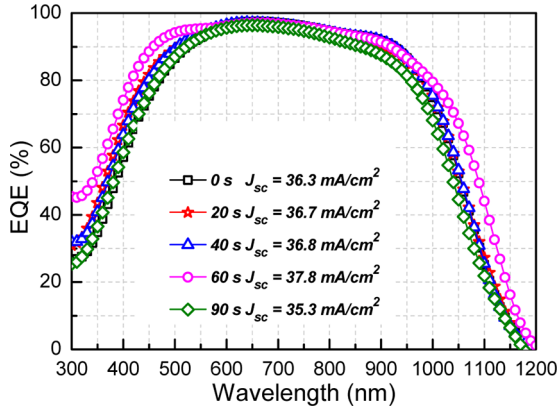

Figure 6. EQE curves of the solar cells prepared with various hydrogen plasma pretreatment durations.

shows the external quantum efficiency (EQE) curves of the solar cells prepared with various hydrogen plasma pretreatment durations. The EQE at short wavelengths has been enhanced

dx.doi.org/10.1021/am5031837 | ACS Appl. Mater. Interfaces 2014, 6, 15098−15104

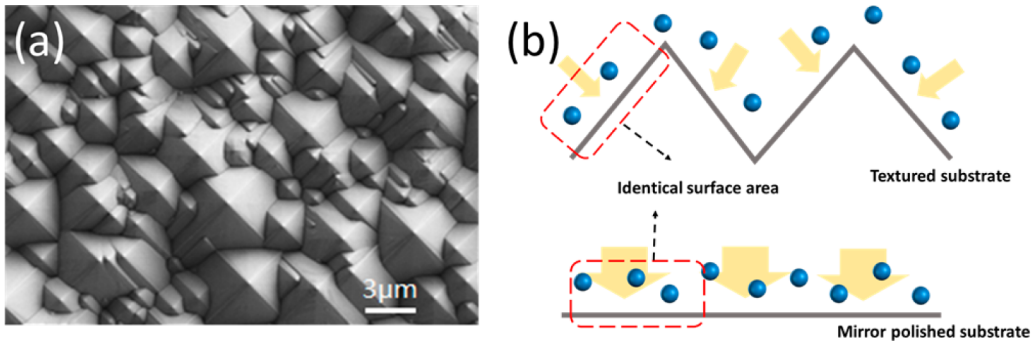

Figure 7. (a) SEM morphology of textured substrate surface. (b) Schematic diagrams depicting hydrogen plasma treatment for textured (top) and polished (bottom) substrates.

for a treatment duration of 60 s, as a result of the improved surface passivation. Moreover, it is worth noting that the long wavelength responses of the solar cells have also been improved. We believe that this is mainly attributable to the fact that the silicon wafers were double-passivated (i-a-Si:H/c-Si/i-a-Si:H); thus, the positive impacts brought by hydrogen plasma pretreatment affected not only the front side but also the rear side of the device.

Nevertheless, we note that the optimal pretreatment duration for SHJ solar cells is ~60 s rather than 40 s, which is the optimal pretreatment duration for a polished wafer. We suggest that the different optimal treatment durations for these two kinds of substrate should be related to the morphologies of their surfaces. Figure 7a shows that the textured c-Si substrates are covered with pyramids to enhance the ability of light trapping, which enlarge the effective surface of the c-Si. For identical glow discharge conditions, the surface of a textured substrate is exposed to a lower average hydrogen plasma density than the surface of a mirror polished substrate; i.e., the larger the surface area, the lower is the plasma density endured by a unit silicon surface, as shown in Figure 7b. Therefore, to achieve the same coverage effects, the hydrogen plasma pretreatment for a textured surface should be longer than that for polished substrates. Collectively, these results indicate that the hydrogen plasma pretreatment will improve the performance of SHJ solar cells based on textured substrates, although the exposure time will need to be prolonged compared with that for treating a polished wafer.

4. CONCLUSIONS

We have obtained high-quality c-Si surface passivation by applying a hydrogen plasma pretreatment process to a silicon wafer before depositing the intrinsic a-Si:H passivation layer. The enhanced passivation effects of hydrogen plasma pretreatment were investigated by using two different methods of measuring minority carrier lifetimes, in combination with ATR-FTIR spectroscopy. Hydrogen plasma treatment for c-Si could modify the microstructure of the resultant a-Si:H films deposited, promote the homogeneity and compactness of the a-Si:H film, and thus improve the τ_{eff}. This is because the hydrogen plasma causes the a-Si:H film precursors (SiH_3) subsequently adsorbed on the surface to achieve energetically favorable (stable) sites, leading to the a-Si:H film formation of an atomically flat surface and improving the passivation level. Finally, by applying the treatment process to the fabrication of SHJ solar cells based on a Cz-textured substrate, we achieved an efficiency of 18.26%.

AUTHOR INFORMATION

Corresponding Author

*E-mail: xdzhang@nankai.edu.cn.

Notes

The authors declare no competing financial interest.

ACKNOWLEDGMENTS

The authors gratefully acknowledge the support from National Basic Research Program of China (Grant Nos. 2011CBA00706, 2011CBA00707), Science and Technology Support Program of Tianjin (12ZCZDGX03600), Major Science and Technology Support Project of Tianjin City (11TXSYGX22100), and Specialized Research Fund for the PhD Program of Higher Education (20120031110039).

REFERENCES

(1) Wang, H.-P.; Lin, T.-Y.; Hsu, C.-W.; Tsai, M.-L.; Huang, C.-H.; Wei, W.-R.; Huang, M.-Y.; Chien, Y.-J.; Yang, P.-C.; Liu, C.-W.; Chou, L.-J.; He, J.-H. Realizing High-Efficiency Omnidirectional n-Type Si Solar Cells via the Hierarchical Architecture Concept with Radial Junctions. *ACS Nano* **2013**, *7*, 9325−9335.

(2) Hsiao, J.-C.; Chen, C.-H.; Lin, C.-C.; Wu, D.-C.; Yu, P. Effect of Hydrogen Dilution on the Intrinsic a-Si:H Film of the Heterojunction Silicon-Based Solar Cell. *J. Electrochem. Soc.* **2011**, *158*, H876.

(3) Wang, H.-P.; Lin, T.-Y.; Tsai, M.-L.; Tu, W.-C.; Huang, M.-Y.; Liu, C.-W.; Chueh, Y.-L.; He, J.-H. Toward Efficient and Omnidirectional n-Type Si Solar Cells: Concurrent Improvement in Optical and Electrical Characteristics by Employing Microscale Hierarchical Structures. *ACS Nano* **2014**, *8*, 2959−2969.

(4) Lin, C. H.; Tsai, T. H.; Wang, C. M.; Yeh, W. T. Photodetectors with an HIT Structure on p-type Crystalline Si Wafers. *Appl. Surf. Sci.* **2013**, *275*, 269−272.

(5) Gharghi, M.; Fathi, E.; Kante, B.; Sivoththaman, S.; Zhang, X. Heterojunction Silicon Microwire Solar Cells. *Nano Lett.* **2012**, *12*, 6278−6282.

(6) Teplin, C. W.; Lee, B. G.; Fanning, T. R.; Wang, J.; Grover, S.; Hasoon, F.; Bauer, R.; Bornstein, J.; Schroeter, P.; Branz, H. M. Pyramidal Light Trapping and Hydrogen Passivation for High-efficiency Heteroepitaxial (100) Crystal Silicon Solar Cells. *Energy Environ. Sci.* **2012**, *5*, 8193.

(7) Hussain, S. Q.; Oh, W.-K.; Ahn, S.; Le, A. H. T.; Kim, S.; Iftiquar, S. M.; Velumani, S.; Lee, Y.; Yi, J. Highly Transparent RF Magnetron-Sputtered Indium Tin Oxide Films for a-Si:H/c-Si Heterojunction Solar Cells Amorphous/Crystalline Silicon. *Mater. Sci. Semicond. Process.* **2014**, *24*, 225−230.

(8) Wang, W. C.; Lin, C. W.; Chen, H. J.; Chang, C. W.; Huang, J. J.; Yang, M. J.; Tjahjono, B.; Huang, J. J.; Hsu, W. C.; Chen, M. J. Surface Passivation of Efficient Nanotextured Black Silicon Solar Cells Using Thermal Atomic Layer Deposition. *ACS Appl. Mater. Interfaces* **2013**, *5*, 9752−9759.

(9) Liang, Z.; Cai, X.; Tan, S.; Yang, P.; Zhang, L.; Yu, X.; Chen, K.; Zhu, H.; Liu, P.; Mai, W. Fabrication of n-Type ZnO Nanowire/Graphene/p-Type Silicon Hybrid Structures and Electrical Properties of Heterojunctions. *Phys. Chem. Chem. Phys.* **2012**, *14*, 16111−16114.
(10) Pallarés, J.; Schropp, R. E. I. Role of the Buffer Layer in the Active Junction in Amorphous-Crystalline Silicon Heterojunction Solar Cells. *J. Appl. Phys.* **2000**, *88*, 293.
(11) Jia, Y.; Cao, A.; Kang, F.; Li, P.; Gui, X.; Zhang, L.; Shi, E.; Wei, J.; Wang, K.; Zhu, H.; Wu, D. Strong and Reversible Modulation of Carbon Nanotube-Silicon Heterojunction Solar Cells by an Interfacial Oxide Layer. *Phys. Chem. Chem. Phys.* **2012**, *14*, 8391−8396.
(12) Nemanick, E. J.; Hurley, P. T.; Webb, L. J.; Knapp, D. W.; Michalak, D. J.; Brunschwig, B. S.; Lewis, N. S. Chemical and Electrical Passivation of Single-Crystal Silicon(100) Surfaces through a Two-Step Chlorination/Alkylation Process. *J. Phys. Chem. B* **2006**, *110*, 14770−14778.
(13) Liang, Y.; Xu, Z.; Xia, J.; Tsai, S.-T.; Wu, Y.; Li, G.; Ray, C.; Yu, L. For the Bright Future-Bulk Heterojunction Polymer Solar Cells with Power Conversion Efficiency of 7.4%. *Adv. Mater.* **2010**, *22*, E135−E138.
(14) Herasimenka, S. Y.; Dauksher, W. J.; Bowden, S. G. >750 mV Open Circuit Voltage Measured on 50 μm Thick Silicon Heterojunction Solar Cell. *Appl. Phys. Lett.* **2013**, *103*, 053511.
(15) Lee, K. S.; Yeon, C. B.; Yun, S. J.; Jung, K. H.; Lim, J. W. Improved Surface Passivation Using Dual-Layered a-Si:H for Silicon Heterojunction Solar Cells. *ECS Solid State Lett.* **2014**, *3*, 33−36.
(16) Rahman, M. Z.; Khan, S. I. Advances in Surface Passivation of c-Si Solar Cells. *Mater. Renewable Sustainable Energy* **2012**, *1*, 1−11.
(17) Schulze, T. F.; Korte, L.; Conrad, E.; Schmidt, M.; Rech, B. Electrical Transport Mechanisms in a-Si:H/c-Si Heterojunction Solar Cells. *J. Appl. Phys.* **2010**, *107*, 023711.
(18) Panda, K.; Sankaran, K. J.; Panigrahi, B. K.; Tai, N. H.; Lin, I. N. Direct Observation and Mechanism for Enhanced Electron Emission in Hydrogen Plasma Treated Diamond Nanowire Films. *ACS Appl. Mater. Interfaces* **2014**, DOI: 10.1021/am501398s.
(19) John, P.; Stoikou, M. D. Hydrogen Plasma Interaction with (100) Diamond Surfaces. *Phys. Chem. Chem. Phys.* **2011**, *13*, 11503−11510.
(20) Jimenez-Redondo, M.; Carrasco, E.; Herrero, V. J.; Tanarro, I. Isotopic Exchange Processes in Cold Plasmas of H_2/D_2 Mixtures. *Phys. Chem. Chem. Phys.* **2011**, *13*, 9655−9666.
(21) Martín, I.; Vetter, M.; Orpella, A.; Voz, C.; Puigdollers, J.; Alcubilla, R.; Kharchenko, A. V.; Roca i Cabarrocas, P. Improvement of Crystalline Silicon Surface Passivation by Hydrogen Plasma Treatment. *Appl. Phys. Lett.* **2004**, *84*, 1474.
(22) Thomas, R. E. Carbon and Oxygen Removal from Silicon (100) Surfaces by Remote Plasma Cleaning Techniques. *J. Vac. Sci. Technol., A* **1992**, *10*, 817.
(23) Anthony, B. In situ Cleaning of Silicon Substrate Surfaces by Remote Plasma-Excited Hydrogen. *J. Vac. Sci. Technol., B: Microelectron. Process. Phenom.* **1989**, *7*, 621.
(24) Kim, Y. D.; Park, S.; Song, J.; Tark, S. J.; Kang, M. G.; Kwon, S.; Yoon, S.; Kim, D. Surface Passivation of Crystalline Silicon Wafer via Hydrogen Plasma Pre-treatment for Solar Cells. *Sol. Energy Mater. Sol. Cells* **2011**, *95*, 73−76.
(25) Thamm, T.; Baumann, W.; Dietrich, D.; Meyer, N.; Stöckel, S.; Marx, G. Preparation of Boron Nitride Thin Films by Microwave PECVD and Their Analytical Characterisation. *Phys. Chem. Chem. Phys.* **2001**, *3*, 5150−5153.
(26) Arnault, J. C.; Petit, T.; Girard, H.; Chavanne, A.; Gesset, C.; Sennour, M.; Chaigneau, M. Surface Chemical Modifications and Surface Reactivity of Nanodiamonds Hydrogenated by CVD Plasma. *Phys. Chem. Chem. Phys.* **2011**, *13*, 11481−11487.
(27) Batra, N.; Vandana; Kumar, S.; Sharma, M.; Srivastava, S. K.; Sharma, P.; Singh, P. K. A Comparative Study of Silicon Surface Passivation Using Ethanolic Iodine and Bromine Solutions. *Sol. Energy Mater. Sol. Cells* **2012**, *100*, 43−47.
(28) Nayak, P.; Singh, B. K. Instrumental Characterization of Clay by XRF, XRD and FTIR. *Bull. Mater. Sci.* **2007**, *30*, 235−238.
(29) Schulze, T. F.; Beushausen, H. N.; Leendertz, C.; Dobrich, A.; Rech, B.; Korte, L. Interplay of Amorphous Silicon Disorder and Hydrogen Content with Interface Defects in Amorphous/Crystalline Silicon Heterojunctions. *Appl. Phys. Lett.* **2010**, *96*, 252102.
(30) Yue, G.; Yan, B.; Sivec, L.; Zhou, Y.; Yang, J.; Guha, S. Effect of Impurities on Performance of Hydrogenated Nanocrystalline Silicon Solar Cells. *Sol. Energy Mater. Sol. Cells* **2012**, *104*, 109−112.
(31) Matsuda, A. Growth Mechanism of Microcrystalline Silicon Obtained from Reactive Plasmas. *Thin Solid Films* **1999**, *337*, 1−6.
(32) Saitoh, K.; Kondo, M.; Fukawa, M.; Nishimiya, T.; Matsuda, A.; Futako, W.; Shimizu, I. Role of the Hydrogen Plasma Treatment in Layer-by-Layer Deposition of Microcrystalline Silicon. *Appl. Phys. Lett.* **1997**, *71*, 3403.
(33) Matsuda, A. Formation Kinetics and Control of Microcrystallite in μc-Si:H from Glow Discharge Plasma. *J. Non-Cryst. Solids* **1983**, *59*−*60*, 767.
(34) Vepřek, S.; Iqbal, Z.; Sarott, F. A. A Thermodynamic Criterion of the Crystalline-to-Amorphous Transition in Silicon. *Philos. Mag. B* **1982**, *45*, 137−145.
(35) Yan, B.; Yue, G.; Yang, J.; Guha, S.; Williamson, D. L.; Han, D.; Jiang, C.-S. Hydrogen Dilution Profiling for Hydrogenated Microcrystalline Silicon Solar Cells. *Appl. Phys. Lett.* **2004**, *85*, 1955.
(36) Chiang, C. M.; Gates, S. M.; Lee, S. S.; Kong, M.; Bent, S. F. Etching, Insertion, and Abstraction Reactions of Atomic Deuterium with Amorphous Silicon Hydride Films. *J. Phys. Chem. B* **1997**, *101*, 9537−9547.
(37) Schüttauf, J.-W. A.; van der Werf, K. H. M.; Kielen, I. M.; van Sark, W. G. J. H. M.; Rath, J. K.; Schropp, R. E. I. High Quality Crystalline Silicon Surface Passivation by Combined Intrinsic and n-Type Hydrogenated Amorphous Silicon. *Appl. Phys. Lett.* **2011**, *99*, 203503.